Vibrational Circular Dichroism: Predominant Conformations and Intermolecular Interactions in (*R*)−(−)-2-Butanol

Feng Wang and Prasad L. Polavarapu*

Department of Chemistry, Vanderbilt University, Nashville, Tennessee 37235

Received: June 27, 2000; In Final Form: September 5, 2000

Vibrational absorption and circular dichroism spectra of (*R*)−(−)-2-butanol have been measured in CS_2 solutions in the 2000−900 cm^{-1} region. Experimental spectra obtained at different concentrations have been compared with the ab initio predictions of absorption and VCD spectra obtained with density functional theory using B3LYP/6-31G* basis set for nine different conformers of (*R*)-2-butanol. The Boltzmann populations, obtained from Gibbs free energies, indicate the presence of all nine conformations for isolated molecule. Vibrational assignments have been proposed with the observed bands assigned mainly for the most stable conformers. The population weighted theoretical spectra are in satisfactory agreement with the experimental spectra obtained at dilute concentrations. The influence of intermolecular hydrogen bonding on the bands originating from C−O−H bending and C−O stretching is observed in the experimental spectra.

Introduction

The absolute configuration of 2-butanol is particularly important in stereochemical relationship since stereochemistry of a large number of compounds have been related to that of 2-butanol and its derivatives.[1] The absolute configuration of chiral 2-butanol was determined by chemical correlation[2a] and NMR spectroscopy,[2b] and (−)-2-butanol was assigned to the (*R*)-configuration. Recently, the conformational preferences of chiral 2-butanol also became an important subject since 2-butanol is used as a model for the O−C−C−C moiety in C-glycosides.[3] However, there are only limited experimental data available on the conformational properties of 2-butanol. Bernstein and Pederson[4a] have measured the specific rotation of 2-butanol as a function of temperature to determine the equilibrium compositions of the conformations. They concluded that anti C−C−C*−C(T) and gauche plus C−C−C*−C(G^+) conformations have the lowest energy, and suggested the population ratio of T, G^+, and G^- conformations as 43:43:14 (see Figure 1 for T, G^+, and G^- structures). In a NMR investigation by Abe et al.,[4b] vicinal H−H coupling constants suggested the population ratio of T, G^+, and G^- conformations as 51: 43: 06; no information was available on the orientation of H−C*−O−H segment. In a recent study on the conformational properties of 2-butanol,[4c] comparison of the MM3 calculated and observed Raman spectra suggested that the stable conformer of liquid 2-butanol has the anti C−C−C*-C conformation (T), but no conclusion with respect to the H−C*−O−H dihedral angle and relative populations of different conformations was obtained.

The combination of experimental and ab initio vibrational optical activity (VOA) spectra has been used in recent years for determining the absolute configuration and predominant conformations of chiral molecules in the solution phase.[5−6] Vibrational circular dichroism (VCD) and vibrational Raman optical activity (VROA) are two different branches of VOA. The utility of VCD for structural elucidation is facilitated by two advances: (a) improvements in VCD instrumentation have made it possible to obtain the VCD spectra with enhanced signal-to-noise ratio and (b) ab initio applications using density functional theory (DFT)[7] have become state-of-the-art in recent years. The DFT theory, which provides vibrational frequencies and intensities that are comparable to the post-SCF calculations employing electron correlation, has also been extended to the VCD intensity calculations[8] and implemented in standard software.[9] These developments make it possible to use VCD for reliable determination of the absolute configuration and predominant conformations in the solution phase.

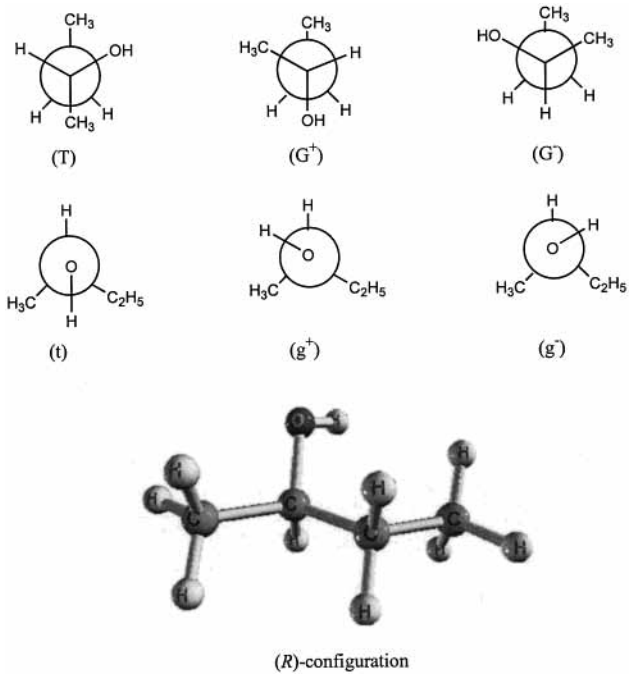

Figure 1. Different conformations of (*R*)-2-butanol, based on the differences of the dihedral angles C−C−C*−C and H−C*−O−H.

Vibrational circular dichroism of α-deuterioethanol[10] (the smallest chiral alcohol) has been studied to obtain the information on predominant conformations and absolute configuration successfully. 2-butanol represents the smallest chiral molecule among the alcohols that do not have isotopic substituents. The

10.1021/jp0022914 CCC: $19.00
Published on Web 10/21/2000

TABLE 1: Conformations and Energies of (*R*)-2-butanol

	starting geometry[b]		converged geometry[b]		energy[c]				
label[a]	CCC*C	HC*OH	CCC*C	HC*OH	electronic	Gibbs	ΔE[d]	population[e] (%)	dipole[f] moment
(T,t)	180	180	177.2	178.9	−233.667 443	−233.559 869	0	0.289	1.5860
(T,g$^+$)	180	60	177.2	60.3	−233.667 138	−233.559 575	0.184	0.211	1.5092
(T,g$^-$)	180	−60	−179.4	−55.8	−233.666 925	−233.559 403	0.292	0.176	1.5817
(G$^+$,t)	60	180	64.3	179.9	−233.666 255	−233.558 687	0.742	0.083	1.6374
(G$^+$,g$^-$)	60	−60	65.1	−63.98	−233.666 201	−233.558 607	0.792	0.076	1.5938
(G$^+$,g$^+$)	60	60	66.3	64.8	−233.666 060	−233.558 514	0.850	0.069	1.4950
(G$^-$,g$^-$)	−60	−60	−61.2	−61.3	−233.665 837	−233.557 995	1.176	0.039	1.5159
(G$^-$,g$^+$)	−60	60	−61.2	65.8	−233.665 577	−233.557 762	1.322	0.031	1.5105
(G$^-$,t)	−60	180	−64.6	173.2	−233.665 468	−233.557 624	1.409	0.027	1.6392

[a] See Figure 1 for labels. [b] Dihedral angle. [c] In Hartrees. [d] Relative energy difference between Gibbs energies, in kcal/mol. [e] Population based on Gibbs energies. [f] In Debye.

absolute configuration of 2-butanol has not yet been confirmed by spectroscopic techniques; moreover very little information (vide supra) is available on the predominant conformations of 2-butanol in solution phase. It is useful to have the experimental and theoretical data that would identify the absolute configuration of, and predominant conformations preferred by, 2-butanol.

Interactions between molecules have significant influence on their conformational stability, especially for molecules that participate in intra- and intermolecular hydrogen bonding, dipole−dipole interactions, and dipole−induced dipole interaction.[11−12] Influence of concentration and solvent on the conformational stability of (*S*)−(−)-3-butyn-2-ol[11] and (S)−(+)-epichlorohydrin[12] have been studied recently. Unlike in (*S*)−(−)-3-butyn-2-ol and (S)−(+)-epichlorohydrin, there is neither intramolecular hydrogen bonding nor large difference in the dipole moments among different conformations of chiral 2-butanol. The changes in vibrational absorption and VCD spectra with concentration, in general, may come from (a) the influence of intermolecular hydrogen bonding on structural parameters, and hence on force constants in different conformations, (b) the influence of intermolecular interactions (such as hydrogen bonding, dipole−dipole interaction, and dipole−induced dipole interaction) on the relative conformation populations, which results in the population weighted spectra to be different. In the case of chiral 2-butanol, it is not clear if either one or both of these two sources prevail and result in variations in absorption and VCD spectra as a function of concentration. Vibrational absorption and VCD spectra of (−)-2-butanol are investigated here to determine its absolute configuration, equilibrium composition of conformers in dilute solutions, and the influence of intermolecular interactions on conformer compositions.

TABLE 2: Comparison of Predicted and Observed Frequencies for (*R*)−(−)-2-butanol

band no.[a]	exptl (cm^{-1})[b]	predicted (cm^{-1})[c]	calcd (cm^{-1})[d]	assignment
1	1373	1387	1443	CC*H bending
		1381	1437	CC*H bending
2	1349	1353	1407	C*CH bending
		1349	1403	OC*H bending
3	1319	1315	1368	CC*H bending
4	1297	1302	1354	C*CH bending
5	1289	1285	1337	C*CH bending
6	1265	1262	1313	CC*H bending
7	1241	1238	1288	COH bending
		1226	1275	COH bending
		1216	1265	COH bending
8	1156	1146	1192	C*CH bending
9	1143	1136	1182	C*CH bending, CO stretching
10	1127	1124	1169	C*CH bending, CO stretching
11	1112	1110	1155	C*CH bending, CO stretching
12	1096	1097	1141	CC stretching
13	1076	1058	1101	COH bending, CCH bending
14	1029	1011	1052	CC stretching
15	989	989	1029	CCH bending
		971	1010	CCH bending
16	966	953	991	C*CH bending
17	910	895	931	C*CH bending
		890	926	C*CH bending

[a] The number is the same as that in Figures 4 and 5. [b] Experimental Frequencies collected at concentration of 0.029 M. [c] Band positions from the simulated spectra with populations given in Table 1, scaled ab intio calculations with scaling factor of 0.9613. [d] Unscaled ab initio band positions from population weighted spectra.

Procedures

(−)-2-butanol was purchased from Aldrich Chemical Co. The infrared and VCD spectra were recorded on a commercial Fourier transform VCD spectrometer, Chiralir (Bomem-BioTools, Canada) with a ZnSe beam splitter, BaF_2 polarizer, optical filter (transmitting below 2000 cm^{-1}) and a 2 × 2 mm HgCdTe detector. One difference from the standard Chiralir instrument is that the photo elastic modulator used was a PEM-80 model (Hinds Instruments) without AR coating on the ZnSe optical element. The VCD spectra were recorded, using the supplied Chiralir software, with 3 h data collection time at 4 cm^{-1} resolution. The transmission properties of optical filter and BaF_2 substrates used in the instrument restrict the range of measurements to 2000−900 cm^{-1}. Spectra were measured in CS_2 solvent at five different concentrations, 0.029, 0.089, 0.347, 0.789, and 2.213 M at path length of ∼4500, ∼1560, ∼360, ∼160, or ∼60 μm, respectively. The sample was held in a variable path length cell with BaF_2 windows. In the presented absorption spectra, the solvent absorption was subtracted out. In the presented VCD spectra, the raw VCD spectrum of the solvent was subtracted. The spectra obtained at 0.029 M and 0.089 M concentrations are almost identical, so the spectra at 0.089 M are not shown here. Spectra of the neat liquid were also measured and the sample was held in a fixed path length cell (6 μm) with BaF_2 windows.

The ab initio vibrational frequencies, absorption, and VCD intensities for (*R*)-2-butanol were calculated using Gaussian 98 program[9] on a Pentium II 300 MHz PC. The calculations used the density functional theory (DFT) with B3LYP functional[7,13] and 6-31G* basis set.[14] The procedure for calculating the VCD intensities using DFT theory is due to Cheeseman et al.[8] as implemented in Gaussian 98 program.[9] The theoretical absorption and VCD spectra were simulated with Lorentzian band shapes and 8 cm^{-1} full width at half-height. Since the ab initio

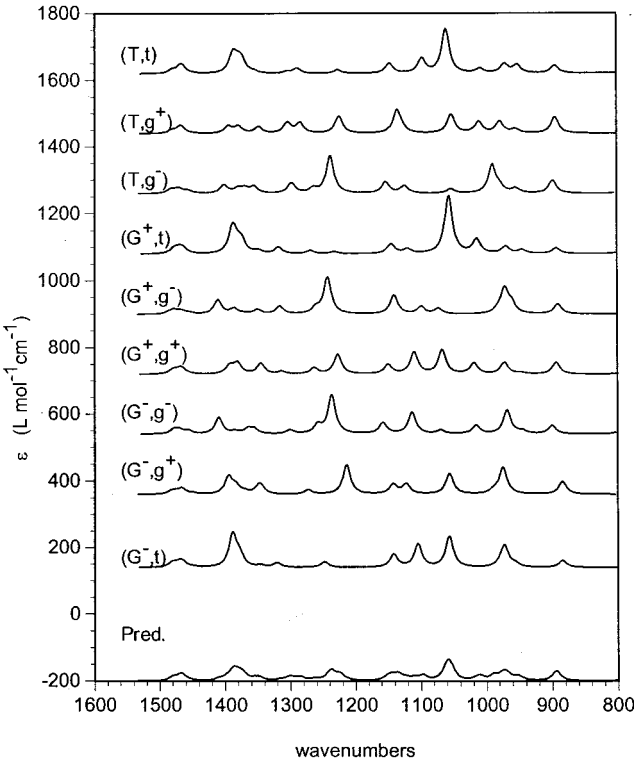

Figure 2. Ab initio vibrational absorption spectra for nine conformers of (*R*)-2-butanol obtained with B3LYP/6-31G* basis set. The spectra were simulated with Lorentzian band shapes and 8 cm^{-1} half-widths, and frequencies were multiplied with 0.96. The labels on the traces are the conformation labels (Figure 1). The predicted spectrum (bottom trace) is obtained by adding the population weighted absorption spectra of all conformers.

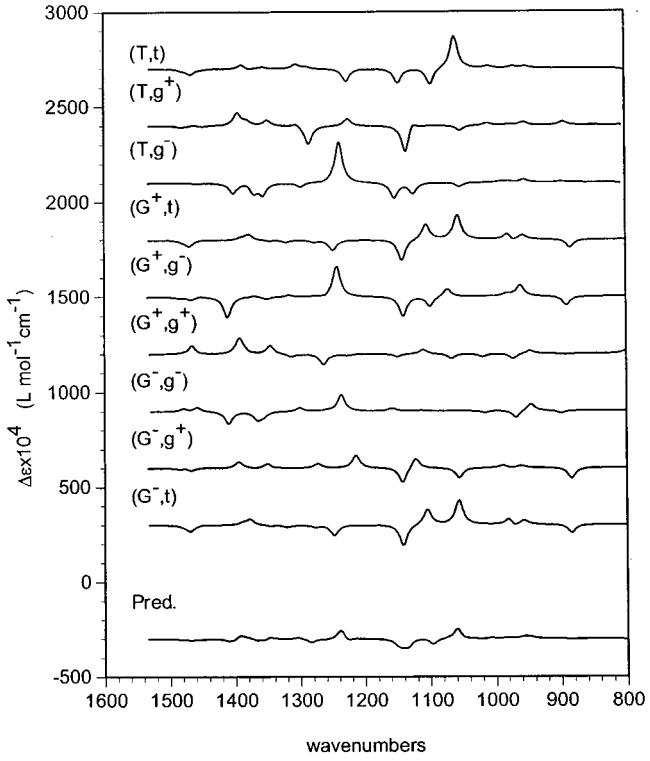

Figure 3. Ab initio VCD spectra for nine conformers of (*R*)-2-butanol obtained with B3LYP/6-31G* basis set. The spectra were simulated with Lorentzian band shapes and 8 cm^{-1} half-widths and frequencies were multiplied with 0.96. The labels on the traces are the conformation labels (Figure 1). The predicted spectrum (bottom trace) is obtained by adding the population weighted VCD spectra of all conformers.

predicted band positions are higher than the experimental values, the ab initio frequencies have been scaled with 0.96.

For the normal coordinate analysis, the following procedure has been used to transform the ab initio results into a form required for our normal coordinate analysis programs. The Cartesian coordinates obtained for the optimized structure were input into the **G**-matrix program[15] together with the complete set of 39 internal coordinates. The **B**-matrix in the output was then used to convert the ab initio force field in Cartesian coordinates to a force field in the desired internal coordinates for all conformers. The internal coordinate force constants were then input, along with the **B**-matrix into the vibrational optical activity program developed in our laboratory to calculate the potential energy distribution (PED), for all conformers.

Results and Discussion

Nine possible conformations of (*R*)-2-butanol (see Figure 1 and Table 1), differing in the dihedral angle C−C−C*−C (labeled as T, G^+, and G^-) and H−C*−O−H (labeled as t, g^+, g^-), are investigated. The geometries were optimized with B3LYP/6-31G* basis set. The converged C−C−C*-C and H−C*-O−H dihedral angles, optimized energies and relative populations based on the Gibbs free energies are listed in Table 1. Although anti C−C−C*-C conformations are more stable than gauche C−C−C*-C conformations, their Gibbs energy differences are not very large, so gauche C−C−C*-C conformations cannot be neglected. The most stable conformation is that labeled as (T, t); The MM3 result[4c] suggested that an averaged conformation of (T, g^+) and (T, t) is the most stable one. For the next most stable conformation, MM3 result[4c] suggested (G^+, t) conformation, while the present results suggest (T, g^-) conformation. On the basis of the calculated dipole moments, for a given C−C−C*-C orientation, anti H−C*-O−H conformation (*t*) would be favored over g^+ and g^- conformations at higher concentrations, but the differences in their dipole moments are not large enough to have a significant impact on the relative conformation populations.

All nine conformers investigated are found to have energy minima (all vibrational frequencies are real) at the B3LYP/6-31G* level, so the absorption and VCD intensities have been calculated for all of them at the B3LYP/6-31G* level. In Table 2, the calculated frequencies come from the population weighted theoretical spectra and the observed bands are assigned predominantly for the (T, t), (T, g^+), and (T, g^-) conformers. The predicted frequencies match the observed data very well. The predicted absorption and VCD spectra simulated with 8 cm^{-1} half-widths and Lorentzian band shapes are shown in Figures 2 and 3. The vibrational frequencies obtained in B3LYP/6-31G* calculation have been multiplied with 0.96. These theoretical spectra can be compared (Figures 4-5) to the experimental spectra of (−)-2-butanol at different concentrations.

The experimental absorption spectrum at lower concentration contains seventeen bands at ∼1373, 1349, 1319, 1297, 1289, 1265, 1241, 1156, 1143, 1127, 1112, 1096, 1076, 1029, 989, 966, and 910 cm^{-1} in the 1400−900 cm^{-1} region. As the concentration is increased, relative intensities of bands at 1076(#13) and 1241(#7) cm^{-1} (which are assigned to C−O−H bending vibration) decrease and shift to higher frequencies while the relative intensities of bands at 1096(#12), 1112(#11), 1127(#10), 1289(#5), 1297(#4), and 1319(#3) cm^{-1} increase; the difference between the relative intensities of bands at 1156(#8) and 1143(#9) cm^{-1} becomes small. The intermolecular hydrogen bonding makes the C−O−H bending and C−O stretching vibrations shift to higher frequencies due to the

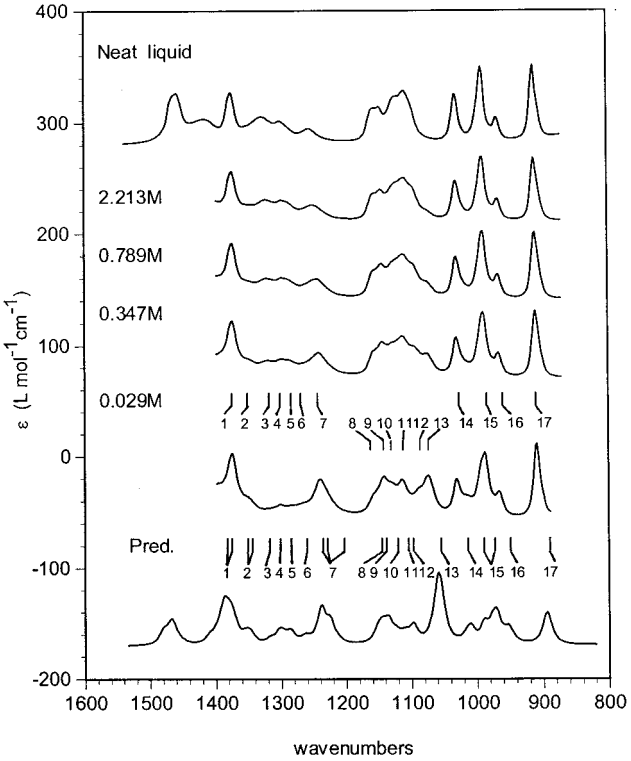

Figure 4. Comparison of the experimental absorption spectra of (−)-2-butanol at different concentrations (top five traces) with the predicted (population weighted) absorption (bottom trace) obtained with B3LYP/6-31G* basis set. The spectra were simulated with Lorentzian band shapes and 8 cm^{-1} half-widths, and frequencies were multiplied with 0.96. The labels on the top five traces give concentration employed for the experimental spectra. The labels for the peaks are the same as those in Table 2.

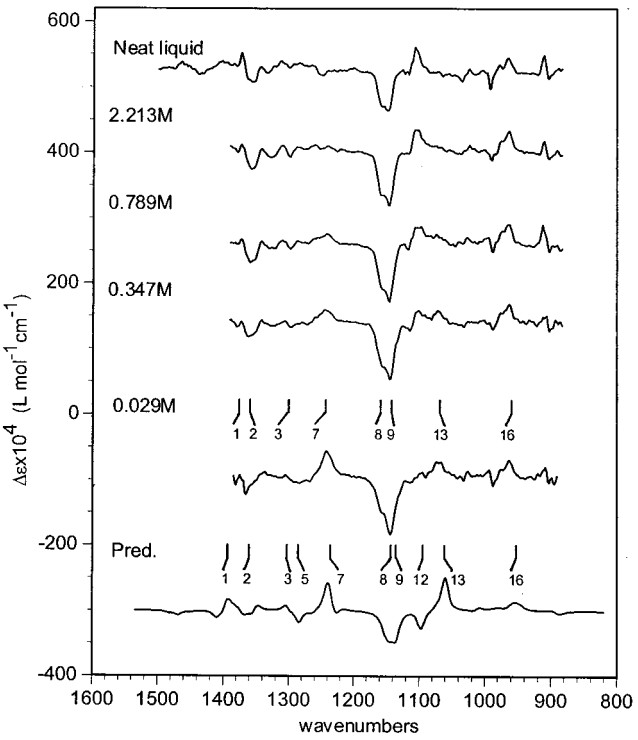

Figure 5. Comparison of the experimental VCD spectra of (−)-2-butanol at different concentrations (top five traces) with the VCD predicted (population weighted) for (R)-2-butanol (bottom trace) using B3LYP/6-31G* basis set. The spectra were simulated with Lorentzian band shapes and 8 cm^{-1} half-widths and frequencies were multiplied with 0.96. The labels on the top five traces give concentration employed for the experimental spectra. The labels for the peaks are the same as those in Table 2.

changes in force constants upon hydrogen bonding.[16] This reasoning is reflected in the shift of 1076(#13) and 1241(#7) cm^{-1} band to higher frequencies and the shift of 1143(#9) to 1156(#8) cm^{-1} as the concentration is increased. At lower concentrations, intermolecular hydrogen bonding is expected to be less significant, so the experimental spectra at lower concentrations are expected to be closer to those predicted for isolated molecules. This in fact is evident in Figure 4, where the population weighted theoretical absorption spectrum compares more favorably to the experimental absorption spectrum obtained at 0.029 M concentration. Nevertheless the intermolecular hydrogen bonding is still significant even in dilute solution as reflected by the difference in relative intensities between bands 1076(#13) and 1241(#7) cm^{-1} in experimental absorption spectrum (0.029 M) and corresponding bands at 1058(#13) and 1238(#7) cm^{-1} in predicted spectrum. However, there are not considerable differences in relative intensities of the band at 1373(#1) cm^{-1} and the group of bands at 1029(#14), 989(#15), 966(#16), and 910(#17) cm^{-1} with the change of concentration, which indicates that there are not significant differences in conformational populations at different concentrations, because these bands should be sensitive to the change of populations of conformations (see Figure 2).

The experimental VCD spectrum at concentration of 0.029 M shows six bands at 1246(+), 1156(−), 1145(−), 1072(+), 988(−), and 963(+) cm^{-1}. As the concentration is increased the intensities of positive VCD bands at 1246(#7) and 1072(#13) cm^{-1} (C−O−H bending) decrease, and a new positive band at 1101 cm^{-1} appears and increases. The population weighted theoretical VCD spectrum matches better with the experimental VCD spectrum obtained at 0.029 M concentration. The differences between predicted and experimental (0.029 M) VCD spectra suggest that the intermolecular hydrogen bonding is present even at dilute concentrations. The shift to higher frequencies of the positive bands at 1072(#13) and 1246 cm^{-1}(#7) makes the negative bands (corresponding to 1097(#12) and 1285 (#5) cm^{-1} in the predicted VCD spectrum) vanish in experimental VCD spectrum. In addition, the difference between the relative intensities of the negative bands at 1143(#9) and 1156 cm^{-1} (#8) becomes small as concentration increases, which indicates the influence of intermolecular hydrogen bonding on C−O stretching vibration. The intensity of band at 966(#16) cm^{-1} remains almost the same at different concentrations, indicating that intermolecular hydrogen bonding may not have a significant influence on the composition of the conformations for chiral 2-butanol in solution phase.

Thus, based on the absorption and VCD spectra obtained at different concentrations, and the corresponding to theoretical spectra, it appears that the relative populations predicted for isolated (*R*)-2-butanol are applicable to the solution phase sample at lower concentrations. At higher concentrations, because of the influence of intermolecular bonding on C−O−H bending and C−O stretching, there are corresponding shifts in the vibrational absorption and VCD spectra. Conformational composition does not appear to change with concentration for 2-butanol, which is supported by small differences in dipole moments of the conformations.

The experimental absorption and VCD spectra of the neat liquid (Figures 4-5) are consistent with the obtained results for (−)-2-butanol at high concentration. The temperature influence (20−60 °C) on the absorption and VCD spectra has also been studied. Minor differences in the ranges for O−H stretching,

C−O stretching and C−O−H bending vibrations have been observed, but the differences are too small for further investigations.

Summary

The comparison of experimental and ab initio predicted absorption and VCD spectra indicate that (a) (−)-2-butanol is of *R*-configuration; (b) the Gibbs energies of different conformations are closely spaced and all nine conformations of (R)-2-butanol are present in solution phases; (c) anti C−C−C−C conformations (T) are the most stable conformations; (d) while there is neither intramolecular hydrogen bonding nor significant difference in dipole moment among different conformations of 2-butanol, intermolecular hydrogen bonding makes the bands assigned to C−O−H bending and C−O stretching shift to higher frequencies, but its influence on the conformational composition of chiral 2-butanol is small.

Acknowledgment. Grants from the National Science Foundation (CHE9707773) and Vanderbilt University are gratefully acknowledged.

References and Notes

(1) Wiberg, K. B. *J. Am. Chem. Soc*. **1952**, *74*, 3891.

(2) (a) Levene, P. A.; Walti, A.; Haller, H. L. *J. Biol. Chem*. **1927**, *71*, 465. (b) Harada, K.; Shimizu, Y.; Kawakami, A.; Fujii, K. *Tetrahedron Lett*. **1999**, *40*, 9081.

(3) Houk, K. N.; Eksterowicz, J. E.; Wu, Y. D.; Fuglesang, C. D.; Mitchell, D. B. *J. Am. Chem. Soc*. **1993**, *115*, 4170.

(4) (a) Bernstein, H. J.; Pederson, E. E. *J. Chem. Phys*. **1949**, *17*, 885. (b) Abe, K.; Ito, K.; Sueyawa, H.; Hirota, M.; Nishio, M. *Bull. Chem. Soc. Jpn*. **1986**, *59*, 3125. (c) Hagemann, H.; Mareda, J.; Chiancone, C.; Bill, H. *J. Mol. Struct*. **1997**, *410*, 357.

(5) Polavarapu, P. L.; Zhao, C.; Ramig, K. *Tetrahedron: Asymmetry* **1999**, *10*, 1099. Polavarapu, P. L.; Cholli, A.; Vernice, G. *J. Am. Chem. Soc*. **1992**, *114*, 10953. Polavarapu, P. L.; Zhao, C.; Cholli, A. L.; Vernice, G. *J. Phys. chem*. **1999**, *103*, 6127.

(6) Costante, J.; Hecht, L.; Polavarapu, P. L.; Collet, A.; Barron, L. D. *Angew. Chem. Int. Ed*. **1997**, *36*, 885; Ashvar, C. S.; Devlin, F. J.; Stephens, P. J. *J. Am. Chem. Soc*. **1999**, *121*, 2836.

(7) Becke, A. D. *J. Chem. Phys*. **1993**, *98*, 1372, 5648.

(8) Cheeseman, J. R.; Frisch, M. J.; Devlin, F. J.; Stephens, P. J. *Chem. Phys. Lett*. **1996**, *252*, 211.

(9) Frisch, M. J.; Trucks, G. W.; Schlegel, H. B.; Scuseria, G. E.; Robb, M. A.; Cheeseman, J. R.; Zakrzewski, V. G.; Montgomery, J. A., Jr.; Stratmann, R. E.; Burant, J. C.; Dapprich, S.; Millam, J. M.; Daniels, A. D.; Kudin, K. N.; Strain, M. C.; Farkas, O.; Tomasi, J.; Barone, V.; Cossi, M.; Cammi, R.; Mennucci, B.; Pomelli, C.; Adamo, C.; Clifford, S.; Ochterski, J.; Petersson, G. A.; Ayala, P. Y.; Cui, Q.; Morokuma, K.; Malick, D. K.; Rabuck, A. D.; Raghavachari, K.; Foresman, J. B.; Cioslowski, J.; Ortiz, J. V.; Stefanov, B. B.; Liu, G.; Liashenko, A.; Piskorz, P.; Komaromi, I.; Gomperts, R.; Martin, R. L.; Fox, D. J.; Keith, T.; Al-Laham, M. A.; Peng, C. Y.; Nanayakkara, A.; Gonzalez, C.; Challacombe, M.; Gill, P. M. W.; Johnson, B.; Chen, W.; Wong, M. W.; Andres, J. L.; Gonzalez, C.; Head-Gordon, M.; Replogle, E. S.; Pople, J. A. *Gaussian 98*, Revision A.3; Gaussian, Inc.: Pittsburgh, PA, 1998.

(10) (a) Dothe, H.; Lowe, M. A.; Alper, J. S. *J. Phys. Chem*. **1989**, *93*, 6632. (b) Shaw, R. A.; Wieser, H.; Dutler, R.; Rauk, A. *J. Am. Chem. Soc*. **1990**, *112*, 5401.

(11) Wang, F.; Polavarapu, P. L. *J. Phys. Chem*. **2000**, *104*, 1822.

(12) Wang, F.; Polavarapu, P. L. *J. Phys. Chem*. **2000**, *104*, 6189.

(13) Becke, A. D. *Phys. Rev. A* **1988**, *38*, 3098.

(14) Hehre, W. J.; Radom, L.; Schleyer, P. V. R.; Pople, J. A. *Ab initio Molecular Orbital Theory*; John Wiley & Sons: New York, 1986.

(15) Schachtschneider, J. H. Vibrational Analysis of Polyatomic Molecules. Reports 231/64 and 57/65; Shell Development Co.: Houston, TX, 1962.

(16) Sun, Z.; Wang, F.; Tang, Z.; Yan, G. *Chin. J. At. Mol. Phys*. **1995**, *12*, 375. Lozynski, M.; Roszak, D. R.; Mack, H.-G. *J. Phys. Chem. A*, **1998**, *102*, 2899.